Tribology International 101 (2016) 59–68

Contents lists available at ScienceDirect

Tribology International

journal homepage: www.elsevier.com/locate/triboint

Running-in and micropitting behaviour of steel surfaces under mixed lubrication conditions ☆

A. Clarke *, I.J.J. Weeks, R.W. Snidle, H.P. Evans

Cardiff School of Engineering, Cardiff University, Wales, United Kingdom

ARTICLE INFO

Article history:
Received 22 November 2015
Received in revised form
9 March 2016
Accepted 10 March 2016
Available online 19 March 2016

Keywords:
Running-in
Mixed lubrication
Roughness

ABSTRACT

The paper investigates the running-in of hardened steel surfaces under mixed lubrication conditions. Pairs of surfaces of both equal and differing hardness were loaded together under rolling/sliding conditions in a twin-disk rig, and the evolution of surface topography was investigated using in-situ profilometry. Evaluation of roughness parameters, height distributions and profile relocation showed that the running-in of these surfaces is a rapid process where the most prominent asperity tips undergo plastic deformation during the initial loading cycles. Finally, the pair of equal hardness disks, following further running in a separate series of experiments, was found to suffer from micro-pitting. This micropitting predominantly occurred along the tips of prominent asperities, and the potential link between running-in and surface failure is discussed.

1. Introduction

When freshly manufactured components are first loaded together in operation, they tend to undergo an initial settling period which is commonly termed ‘running-in’. The running-in phenomenon is specified as a series of processes during which wear rates and friction for lubricated contacts stabilise [1]. These factors are governed by changes in the surface topography due to plastic deformation and mild wear and also chemical changes that may take place both in the lubricant and by tribo-film formation on the contacting surfaces.

It has been known for over a century that proper running-in can greatly lengthen the lifespan of engineering components, though this was not fully understood at the time. When real surfaces initially meet under a condition of no load they first contact at the tips of their asperities [2]. This causes the real area of contact to be far less than the apparent contact area. When load is applied, high pressures will be generated in the region of these micro-contacts and the asperity features will deform plastically until the increased bearing area is sufficient to support the applied load. Although the scenario described is one for dry contact it is also the case for mixed lubrication conditions where the film thickness is of a similar order of magnitude to the composite surface roughness, and aggressive asperities are in direct metallic contact.

The initial period of plastic deformation can modify the subsurface microstructure of the contacting materials, resulting in a degree of work-hardening [3]. However, most investigations have focussed on the geometric changes in the surface topography as this has the most immediate implications for the hydrodynamic performance of the interface.

The geometric change during the running-in of a surface is most frequently described by the use of the average roughness parameter (Ra). Though used liberally it does not provide any information regarding the shapes of the asperities [4]. Whitehouse and Archard [5] set out to quantify the surface roughness using various statistical parameters that had not been previously employed as descriptors of topography. They considered the mean radius of curvature of the asperity tips to be an important descriptor of a profile measurement. It was found that when subjected to loading, surface measurements show a rapid increase in radius of curvature of asperities as they deform [6]. When operating under elastohydrodynamic lubrication (EHL) conditions, this change allows for more effective lubrication as a result of the less severe pressure spikes experienced at each ‘micro-contact’ due to increased conformity as the asperities become more rounded.

Examples of the importance of considering running-in when commissioning new surfaces can be seen in the work of Østvik and Christensen [7] who showed that the load carrying capacity of an EHL contact was greatly improved by running-in and surfaces

☆This paper was presented at the 20th International Colloquium Tribology, Stuttgart/Ostfildern, Germany.

* Corresponding author.
E-mail address: clarkea7@cardiff.ac.uk (A. Clarke).

http://dx.doi.org/10.1016/j.triboint.2016.03.007

subsequently scuffed at higher loads. It was also found that as surfaces ran-in, asperity contacts became less frequent as the highest features were removed or flattened. Early experimental investigations into the running-in of lubricated surfaces tended to refer to the gradual reduction in roughness as a wear process and only hinted towards the plastic deformation of asperity contacts [8]. More recently, the improvement in hydrodynamic performance due to running-in has been demonstrated by the work of Lord and Larsson [9] using the electrical contact method on a variety of test surfaces, where all specimens showed reduced levels of metallic contact once run-in.

The work of Andersson [10] into the running-in of gears explained the flattening of asperities as a wear process. Running-in experiments showed that the lambda ratio, defined as the ratio of film thickness to composite surface roughness, is an important parameter in determining the extent to which the asperity features on engineering surfaces are loaded. Scanning Electron Microscope (SEM) imaging of gear tooth flank replicas showed surface asperity peaks which had been smoothed and flattened as a combined effect of surface yielding and wear, while the valley features remained unchanged, with no modification occurring in the region of the pitch point.

Bishop and Snidle published a number of papers describing their experimental test rig work using circumferentially ground steel disks [11,6,12]. Their experiments showed that as surfaces are loaded together under EHL conditions, asperity features become rapidly flattened in response to increasing load. The mean peak radius of curvature was also seen to increase significantly as more load was applied and the valley features, which were not subject to the same high contact pressures or degree of interaction, retained their shape [6]. Experiments performed to test the effect of surfaces plastically deforming and conforming to one another showed that a hard disk loaded against a less hard disk would leave an imprint of its micro-geometry on the counterface [12] and that the running-in process is essentially one where the micro-geometry of surfaces conform or accommodate each other via rapid plastic deformation. The important implications of conformity of micro-geometry could be seen much earlier in work by Tudor [13], where changing the relative position of two run-in surfaces reduced their hydrodynamic performance. These results suggest that running-in with engineering surfaces is not simply a general flattening of features but an accommodation process where the deformation of asperities is determined by the interaction with corresponding asperities on the counterface.

Lohner et al. [14] investigated the running-in of lubricated line contacts in both gear and disk machine tests. They quantified the effects of lubricant specification on changes in surface roughness parameters and actual surface micro-geometry using profile relocation techniques and, like others, found that the surface modification during running-in was limited to asperity tips.

Recent interest has been directed towards the long term implications of the effect that plastic deformation of asperities has on surface fatigue life. Finite element modelling work conducted by Bryant et al. [15] investigating the plastic deformation of rough surface line contacts draws attention to residual tensile stresses around asperities introduced by plastic deformation. Bryant also demonstrated that the residual rough surface deformation only affects the asperity peaks and does not extend to the valley features.

This paper presents the results of an investigation into running-in under mixed lubrication conditions in a series of disk machine tests. It is shown that under the conditions examined, running-in is essentially a process of plastic deformation where asperities on contacting surfaces rapidly conform to each other. Furthermore, the effects of asperity plastic deformation on the long term fatigue performance of the surface is considered.

2. Power recirculating twin disk test rig

The running-in tests shown here were undertaken using a twin-disk machine, where power is recirculated between the EHL contact and a gear pair, such that the drive motor only has to overcome frictional and other losses in the system. Fig. 1 shows the main components of the test rig.

The test disks are 76.2 mm in diameter and are crowned with a radius of 304.8 mm, giving a self-aligning elliptical point contact with a nominal aspect ratio of 4:1, with the major axis parallel to the shaft. The disks are case hardened to a surface hardness of 800–840 Hv, and are made from a typical alloy gear steel to Rolls-Royce specification 6010. Importantly, the crown is produced using an axial grinding process which gives a surface with directionality similar to that of ground gear teeth in relation to the surface kinematics. The as manufactured surface finish has an average roughness (Ra) between 0.3 and 0.4 μm. The shafts on which the disks are mounted are gear connected, giving a rolling/sliding contact with a slide/roll ratio which depends on the chosen gear ratio. The work presented here used slide/roll ratios of 0.25 and 0.5. The fast shaft rotational speed is steplessly adjustable between 200 and 3000 rpm, and is driven by a 5.5 kW electric motor controlled by a variable frequency drive.

The disks are loaded together hydraulically, allowing the generation of Hertzian maximum contact pressures of up to 2.1 GPa. The contact between the disks is lubricated by jets at both inlet and outlet of the contact, with OEP-80 naval gear lubricant which is a mineral oil with EP additives. OEP-80 is a performance specification, and as such the properties of lubricants meeting that specification can vary, but Oila [16] carried out detailed measurements and found the viscosity at ambient pressure to vary from 0.113 Pa s at 40 °C to 0.031 Pa s at 100 °C, with the pressure-viscosity coefficient (obtained from an empirical viscosity correlation) falling from 2.58×10^{-8} Pa^{-1} to 2.03×10^{-8} Pa^{-1} over the same temperature range.

Traction at the contact is measured via a strain-gauged quill shaft between the drive gearing and the slow shaft. This allows the torque in this shaft to be measured and recorded throughout the experiment. A separate series of runs of the test rig was carried out with the fast shaft disconnected from the power recirculation gears so that the disks ran in a pure rolling configuration. In this means of operation two identical pairs of shaft support bearings provide the frictional resistance to rotation. This can thus be

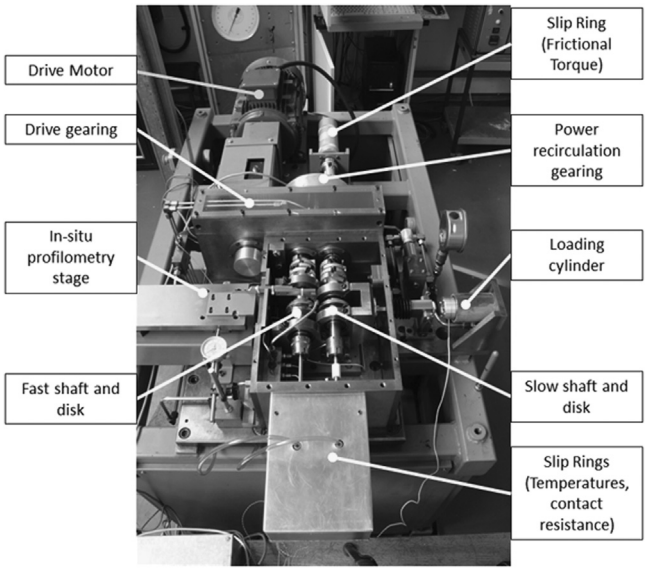

Fig. 1. View of test rig.

measured in terms of the speed, load and temperature. In this way, the bearing friction and windage is carefully calibrated as a function of speed and load, and is used to adjust the total measured friction to give the traction force at the contact. Further details of this procedure are given in [17]. The disk temperatures are measured using thermocouples embedded 3 mm below the disk running tracks, on the axial centre-line. This is achieved by drilling a 2 mm diameter blind hole perpendicular to the face of the disk at a radial position that has a radius 3 mm less than that of the disk. The hole depth is half of the thickness of the disk and a type J thermocouple is potted into the hole using a high conductivity epoxy adhesive to mount the thermocouple in thermal contact with the blind end of the hole. The thermocouple leads are threaded through the hollow shafts to slip rings located in the enclosure labelled as such in Fig. 1. This provides continual measurement of the quasi steady state temperature 3 mm below the surface of each test disk and the mean of these measurements is used to provide a figure for the mean bulk temperature of the disks (and hence lubricant viscosity) as they enter the EHL contact zone.

As described in [18], the slow shaft is electrically isolated from the rest of the rig, and the resistance across the test disks is connected as part of a potential divider circuit, to produce a voltage which varies between 0 mV, when there is significant metallic contact between the disks, and 43 mV when the resistance between the disks is high and the lubrication conditions are essentially full film. The rig also has a stage on which a portable surface profilometer can be mounted (shown in Fig. 1), which allows the profilometer to be aligned accurately with each disk centreline to within 10 μm. This allows the repeated measurement of surface profiles to enable assessment of surface topography at various stages during the running-in process, without having to remove the test disks from the rig. This is an important feature of the rig since removing the disks for measurement would disturb the relative alignment of surface features on the disks, potentially bringing new asperities into contact with each other with consequent additional high contact pressures and further plastic deformation.

3. Running in of surfaces with equal hardness

Experiments were conducted on two test disks with similar measured hardness values of 808 and 819 Hv for the fast and slow disk respectively. The test rig was configured to run at a slide/roll ratio of 0.5 and a fast shaft speed of 1500 rpm, giving a mean entraining velocity of 4.79 m/s and a sliding speed of 2.39 m/s. OEP-80 lubricant at 50 °C was circulated through the rig, with the shafts rotating (with the disks out of contact) to allow the rig to reach the lubricant temperature. Once this had been attained, a load of 4150 N was applied to give a maximum Hertzian contact pressure of 1.7 GPa. This load was applied for 27 s, and then removed and the rig stopped and allowed to cool, before disk surface profiles were measured using the portable profilometer. All profiles presented here were taken on or near the disk's axial centreline and had form and waviness removed using a Gaussian filter with a cut-off wavelength of 0.25 mm, both for relocation and for parameter calculation. Profiles were taken at four circumferential positions around the disk surface, with three axial profiles per position, giving a total of 12 profiles. The profiles were taken on the centre line and on both sides of the centre line with an offset of 0.5 mm. This process was undertaken for two repeated 27 s load stages. During each load stage, the measured contact voltage was approximately 20 mV, indicating mixed lubrication conditions [18] and significant levels of asperity interaction. Following this, the nominally stable surfaces were used in experiments previously reported [18] to investigate mixed lubrication using the electrical contact resistance technique.

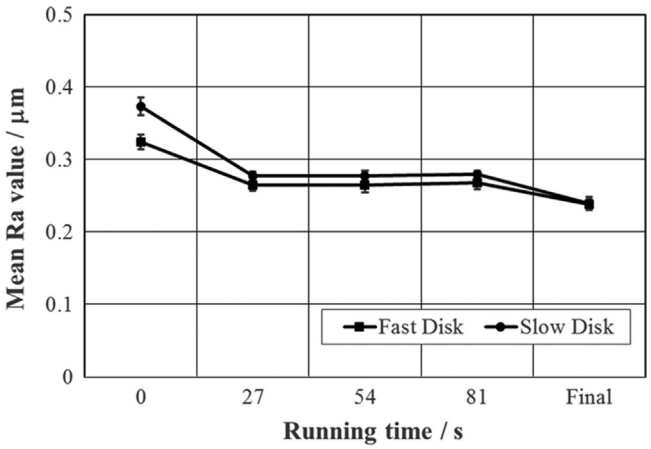

Fig. 2. Mean Ra values for test disks during running-in, with error bars showing ± 1 standard deviation.

Table 1
Evolution of roughness amplitude parameters during running for disks of similar hardness.

Disk	Parameter (μm)	Un-Run	Load Stage 1	Load Stage 2	Load Stage 3	Final
Fast	Rp	0.86	0.50	0.49	0.49	0.42
	Rv	1.29	1.21	1.21	1.25	1.17
	Rz	2.14	1.71	1.70	1.74	1.59
	Ra	0.32	0.27	0.27	0.27	0.24
	Rq	0.41	0.34	0.34	0.34	0.31
Slow	Rp	1.30	0.50	0.50	0.50	0.43
	Rv	1.46	1.37	1.35	1.38	1.35
	Rz	2.76	1.87	1.84	1.89	1.78
	Ra	0.37	0.28	0.28	0.28	0.24
	Rq	0.48	0.36	0.36	0.36	0.32

Fig. 2 shows the mean Ra value (calculated using all profiles measured) for the fast and slow disks before running, at the end of each of the three 27 s load stages, and a final value measured at the conclusion of the mixed lubrication testing reported in [18]. It is clear that both surfaces show a reduction in Ra following initial running, and that no significant change in Ra occurs following the two additional 27 s load stages. On completion of the mixed-lubrication testing, after some 850,000 fast disk rotations the disk surfaces exhibited micropitting-type features, and this is the main cause of the reduction in final Ra.

Using the somewhat crude measure of Ra suggests that the initial surface modification takes place very rapidly, in the first few loading cycles of each asperity, and the surfaces are then stable such that further running (i.e. load stages 2 and 3) under the same loading conditions and similar film thicknesses does not produce further surface modification. This is further confirmed by consideration of a range of roughness parameters, with mean values of the parameters shown in Table 1, calculated using all roughness profiles collected after each load stage).

Table 1 clearly demonstrates that the majority of surface modification takes place during the initial running, with all parameters then being relatively stable following the running-in load stages. There is some final change in parameters measured at the completion of the subsequent mixed lubrication experiments, which is unsurprising given that these tests represented a total of some 850,000 fast disk rotations. The maximum profile peak

height (Rp) shows significant reduction following the first stage of loading, with the fast disk Rp reducing by some 42% to 0.50 μm from an as-manufactured Rp of 0.86 μm. When contrasted to a slight (6%) reduction in maximum valley depth (Rv), it is clear that the modifications to the profile are in the main taking place as asperity tips. It is also clear that, for these surfaces, the majority of changes occur during load stage 1, with only slight variation in parameters measured following load stages 2 and 3.

In order to investigate the nature of the changes occurring to these surfaces further, detailed comparison was made of relocated surface profiles taken after each load stage with ones taken at the same circumferential position on each disk prior to any running. The roughness profiles obtained at each stage were aligned in the profile trace direction so as to minimise the positional error between deep valley features. A constant shift was imposed in the height measurement direction to achieve the best alignment of the deep valley features. Over the 0.5 mm length of the trace comparisons this was found to be an effective method as can be seen in Fig. 3(a) which shows considerable changes to the asperities while the alignment of the deep valley features is reassuringly good. Fig. 3 shows a comparison between the profiles taken after load stage 1 with those taken at the same position on the un-run disks. It can be seen that a significant amount of plastic deformation occurs during the first load stage of both disks. The asperity features become almost uniformly flattened leaving rounded lands. The valley features however are shown to remain relatively unchanged as high localised loads occur predominantly between interacting asperities [19]. In particular, Fig. 3(a) shows a large and isolated asperity at $x=0.125$ mm (labelled A). Taking the valley features of the previous measurements as an acceptable datum point, this prominent feature experiences a change of height of approximately 0.8 μm. Another prominent feature at $x=0.42$ mm (B) has a greater width than the feature occurring at $x=0.125$ mm and does not experience the same level of modification, reducing in height by some 0.3 μm. Similar features on the slow disk shown in Fig. 3(b) are reduced in height, this can be seen where a peak aligned with $x=0.225$ mm (C) is reduced in height by approximately 0.45 μm. In general, prominent asperity features on both surfaces appear to experience a large reduction in height whereas valley regions do not show any significant modification. The rounded nature of the asperity peaks and their rapid modification suggests that this modification process is predominantly one of plastic deformation as opposed to wear.

Fig. 4 shows a similar comparison between another pair of profiles taken after Load Stage 1 and after Load Stage 3. Load Stages 2 and 3 were also of 27 s duration. This shows minimal further surface modification following the changes which occurred during Load Stage 1.

This apparent lack of change between load stages 1 and 3 is perhaps unsurprising considering that, running at a fast disk speed of 1500 rpm, the surfaces have already experienced every possible loading combination at the gear ratio used and come into contact with the same portions of the counterface multiple times. The major asperities remain very closely aligned between measurements, and this demonstrates that plastic deformation occurs in the initial loading cycles of the running-in process. This is consistent with the observations of Jamari and Schipper [20] who showed, using relocated surface profiles, that plastic deformation occurred during the first loading cycles of a rough surface, and Cabanettes and Rosen [21] who used relocated areal measurements to identify running in as being a process predominantly affecting prominent surface features.

It is further instructive to consider the evolution of asperity contact radius with running, for both surfaces. Analysis of the surfaces shown in Figs. 3 and 4 shows that the mean asperity radius before running was 15.7 μm for the fast surface and 16.6 μm for the slow surface. After load stage 1, these mean radii had increased to 73.1 μm and 79.9 μm for the fast and slow surfaces, respectively. At the end of load stage 4, at the conclusion of the running-in experiments, the mean radii were 74.7 μm and 80.3 μm, respectively. Both surfaces therefore experience similar levels of asperity flattening, predominantly occurring during the initial loading cycles.

Using the measurements gathered from the Talysurf profilometer, histograms representing the distribution of surface heights were produced to summarise the data for each load stage. Surface heights were calculated in terms of standard deviations. This was achieved by dividing the surface heights by the standard

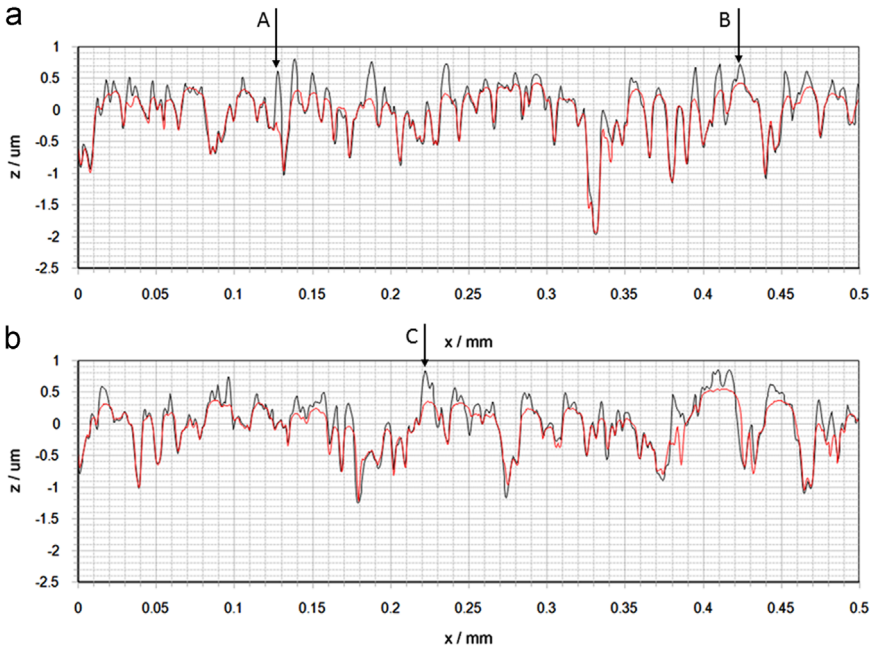

Fig. 3. Profile traces taken from disks in un-run condition (black line) and after load stage 1 (red line) for (a) fast disk and (b) slow disk. (For interpretation of the references to colour in this figure legend, the reader is referred to the web version of this article.)

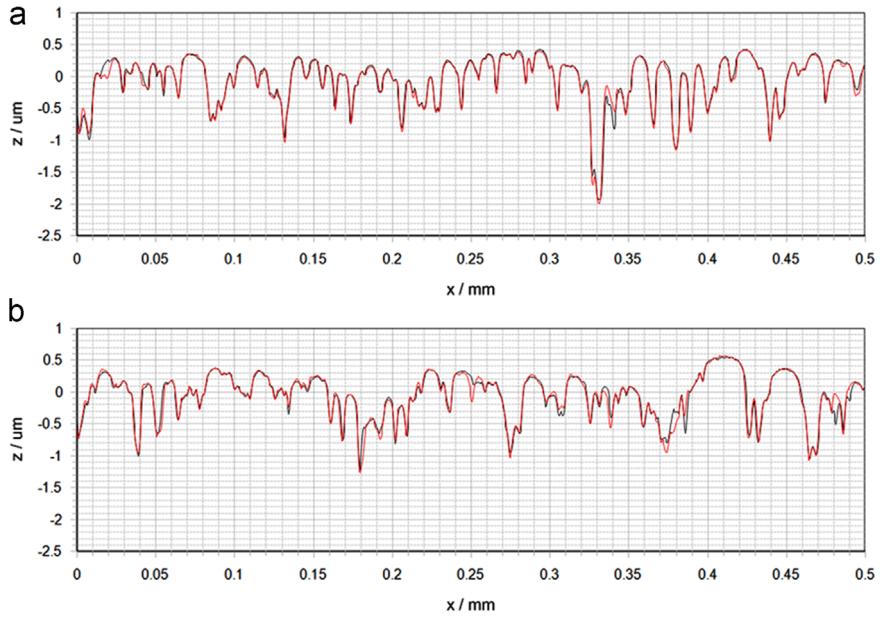

Fig. 4. Profile traces taken from disks after load stage 1 (black line) and after load stage 3 (red line) for (a) fast disk and (b) slow disk. (For interpretation of the references to colour in this figure legend, the reader is referred to the web version of this article.)

Table 2
Roughness distribution data for disks of similar hardness.

Load Stage	Disk	Standard Deviation (μm)	Skewness
Unrun	Fast	0.404	−0.502
	Slow	0.480	−0.135
1	Fast	0.335	−1.066
	Slow	0.357	−1.321
2	Fast	0.335	−1.062
	Slow	0.354	−1.254
3	Fast	0.338	−1.078
	Slow	0.360	−1.325

deviation of all the measured heights for each load stage. Values were then organised into equally sized bins with the distribution normalised and superimposed on a Gaussian distribution curve having the same mean and standard deviation for comparison. For the distributions calculated, the data are shown in Table 2, where it can be seen that over the course of running, the distribution of surface heights is seen to change as asperities become flattened and data becomes more clustered about the mean. The skewness is also included in the table which is a measure of the asymmetry in the height distribution. Distributions become increasingly negatively skewed as a result of the asperity flattening.

Frequency histograms were plotted for the surfaces before running and after each load stage, and are shown in Fig. 5 for the fast disk. The slow disk distributions were very similar to those shown for the fast disk. The un-run distribution shown in Fig. 5 (a) is approximately similar to the superimposed Gaussian distribution, albeit with a small degree of negative skewness. The histogram following load stage 1 is shown for the fast surface in Fig. 5(b). This initial load stage can be seen to further negatively skew the surfaces with asperity peaks becoming deformed and the positive tail of the distribution experiencing a reduction. It can be seen that the negative tail does not change significantly as the surface modification occurs primarily at the asperity tips.

The distribution shown in Fig. 5(c) following load stage 3 demonstrates little sign of modification in comparison to load stage 1 as may be expected given the similarity of the profiles between the load stages. Load stage 3 was the final load stage of the running in process as all measurements indicated that the surface had attained a nominally steady topography under the film thickness and loading conditions experienced.

4. Running-in of surfaces of differing hardness

To provide insight into the effect of surface hardness on the running-in process, a similar running-in test programme was undertaken with two axially ground disks of significantly different hardness values operating under the same load and speed conditions as the disks tested in Section 3. A fast disk with a hardness of 652 Hv and a slow disk with hardness of 801 Hv were used.

For the first load stage, load was applied for a short period of approximately 10 s in order to assess the rapidity at which asperity shapes were modified, in order to quantify the level of plastic deformation that would occur after a brief loading period. Four further load stages, each of 27 s duration, were then carried out in order to better observe any potential wear processes taking place alongside the rapid plastic deformation. The evolution of mean Ra values of the two surfaces is shown in Fig. 6.

It is clear from Fig. 6 that changes in surface roughness are more apparent in the surface of lower hardness, with relatively little change observed in the harder surface. This “smoothing” effect on the less hard surface with the use of oils containing extreme pressure additives was described by Rowe in his investigation into the running-in process in plain bearings [22]. Further comparison of roughness amplitude parameters is shown in Table 3.

It is clear that the changes in roughness parameters are more significant in the less hard (fast) disk than in the harder (slow) disk. It is also clear that, in both disks, changes are concentrated at asperity tips, with large reductions in maximum profile peak height (Rp) compared to the changes in maximum valley depth (Rv).

The effects of the running-in process on the surface topography of both the lower hardness (fast) and higher hardness (slow) surfaces can be seen most clearly by examination of profile measurements. Fig. 7

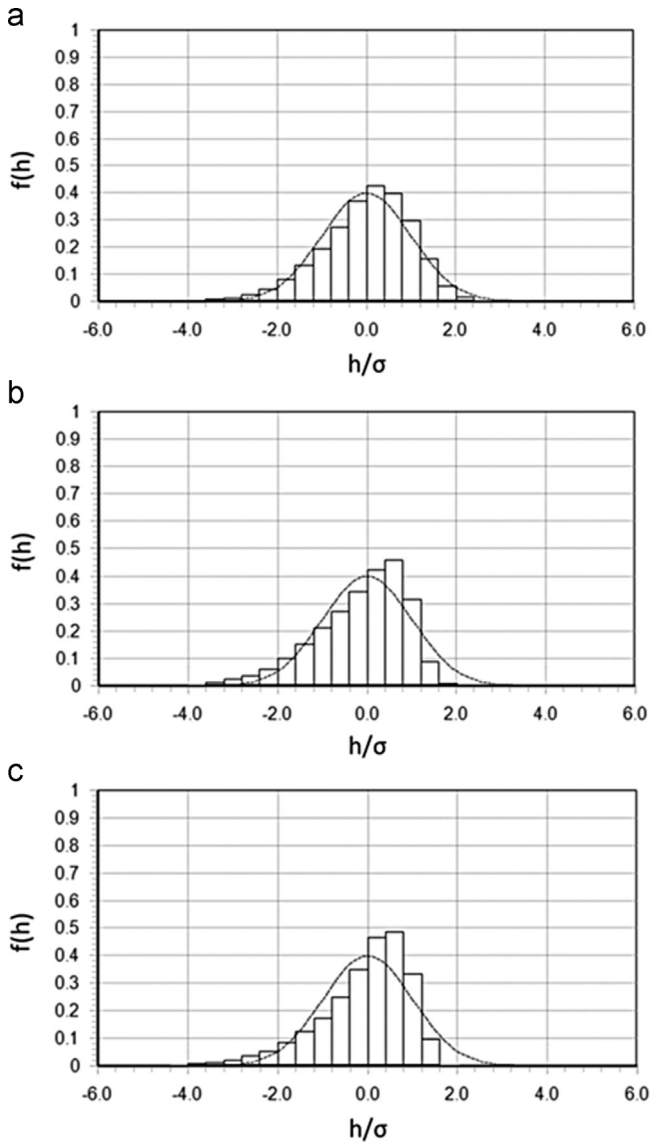

Fig. 5. Histogram of surface heights for fast disk (a) for un-run surface, (b) following load stage 1 and (c) following load stage 3.

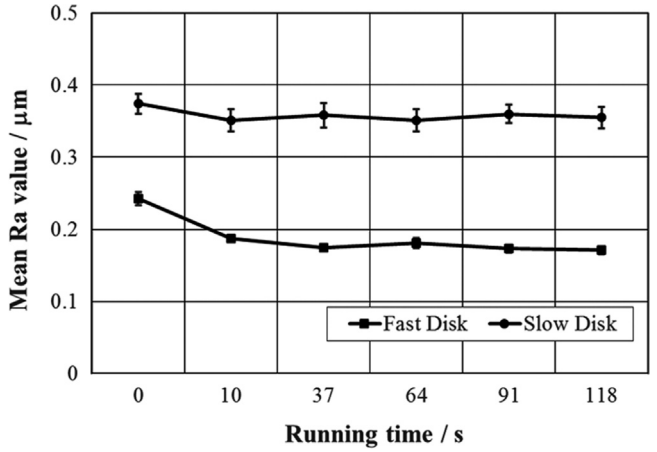

Fig. 6. Ra values for test disks of differing hardness during running-in process.

shows sections of profile taken following load stage 1, superimposed and realigned with the as manufactured profiles for the lower hardness surface in Fig. 7(a) and the higher hardness surface in Fig. 7(b).

Table 3
Evolution of roughness amplitude parameters during running for disks of differing hardness.

Disk	Parameter (μm)	Un-Run	Load Stage 1	Load Stage 2	Load Stage 3	Load Stage 4	Load Stage 5
Fast	Rp	0.61	0.35	0.32	0.37	0.31	0.30
	Rv	0.87	0.80	0.81	0.84	0.80	0.81
	Rz	1.48	1.14	1.12	1.20	1.11	1.12
	Ra	0.24	0.19	0.18	0.18	0.17	0.17
	Rq	0.30	0.23	0.22	0.23	0.22	0.22
Slow	Rp	0.95	0.75	0.75	0.73	0.75	0.73
	Rv	1.53	1.51	1.57	1.50	1.52	1.53
	Rz	2.48	2.26	2.32	2.22	2.26	2.26
	Ra	0.37	0.35	0.36	0.35	0.36	0.36
	Rq	0.48	0.45	0.46	0.44	0.45	0.45

Prominent asperity peaks on the low hardness surface show significant rounding off as they come into contact with portions of the opposing body with smaller scale roughness features also appearing to diminish. Despite this severe deformation occurring on the peaks of the surface, it is clear that the valley features remain undisturbed throughout the loading process, as experiments reported in Section 3 with two hard surfaces have shown. Fig. 7(a) shows asperity features at $x=0.29$ mm (A) and $x=0.34$ mm (B) which experience a reduction in surface height of approximately 0.3 μm and also features with larger tip radii that do not experience the same reduction in height; as seen, for example, at $x=0.43$ mm (C) where an asperity deforms by around 0.1 μm.

In stark contrast to the results seen for the low hardness surface, the slower and harder surface undergoes almost no modification whatsoever – this persistence is clearly visible in Fig. 7(b) where, at the scale shown, even the most prominent peaks remain relatively unmodified. Realigned with their original profiles, it is clear that only the very tips of the hard surface experience any plastic deformation. Examples may be seen in Fig. 7(b) at $x=0.39$ mm (D) and at $x=0.47$ mm (E) where very fine asperity tips experience a change in height of approximately 0.2 μm each following load stage 1. However, some differences may arise from slight axial misalignment, an example of which can be seen at $x=0.45$ mm (F) where the profile representing load stage 1 is briefly seen to exceed that of the un-run measurement. These uncertainties notwithstanding, it is clear that the most significant plastic deformation in these surfaces during the first loading stage occurs on the surface of lower hardness.

Fig. 8 shows aligned pairs of profiles taken after load stage 4 and load stage 5 of the experiments. These show that both surfaces have attained a nominally steady state with very close agreement between both sets of measurements. Changes to the surfaces since the initial load stages appear limited to the fast (lower hardness) disk, where the shorter wavelength roughness features appear to have been largely eliminated. In the subsequent mixed-lubrication experiments [18] these surfaces were found to be stable, except when operated under conditions of thinner films (and hence higher levels of asperity interaction) than the conditions under which this running-in test took place.

Evaluation of the radius of curvature of asperity tips for the surfaces shown in Figs. 8 and 9 shows that the initial radii are different. The harder disk, prior to running, had a mean asperity radius of 16.7 μm which is consistent with the previously evaluated hard disks. The less hard disk has a mean asperity radius of 41.2 μm prior to running, which is significantly higher than that of the harder disks. This is most likely due to the effects of final finishing by grinding being dependant on surface hardness. After load stage 1, the less hard disk had a mean asperity radius of 113.2 μm, whilst the corresponding value for the harder disk was

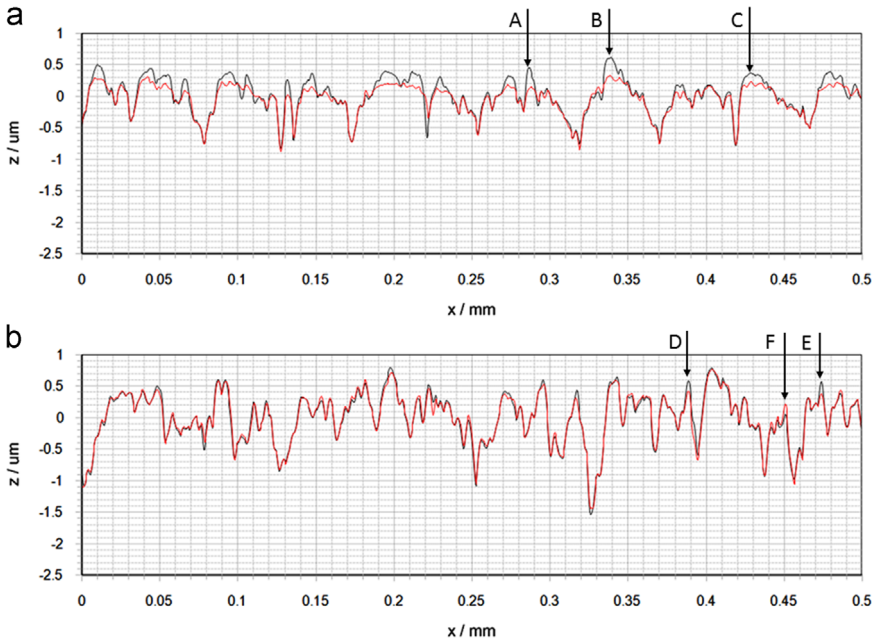

Fig. 7. Profile traces taken from disks in un-run condition (black line) and after load stage 1 (red line) for (a) fast (less hard) disk and (b) slow (harder) disk. (For interpretation of the references to colour in this figure legend, the reader is referred to the web version of this article.)

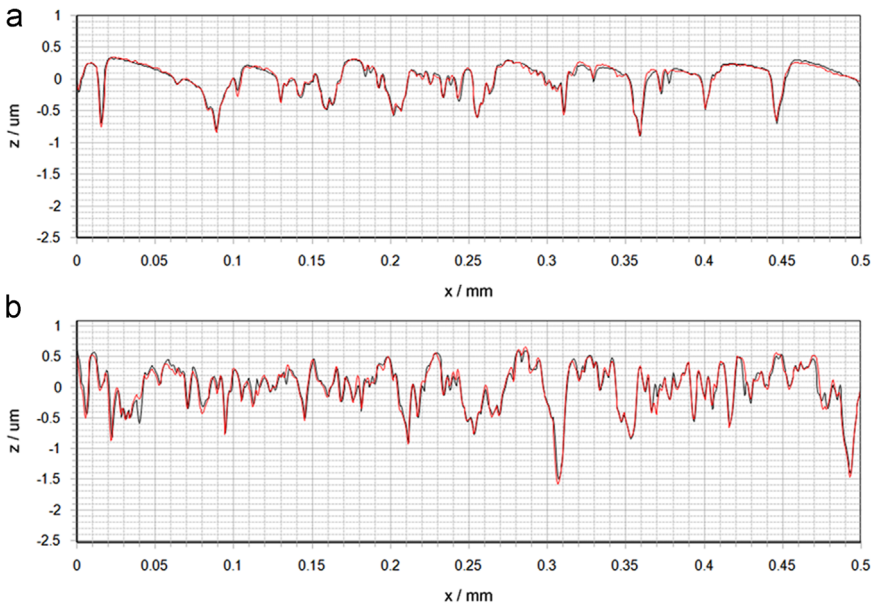

Fig. 8. Profile traces taken from disks after load stage 4 (darker line) and load stage 5 (lighter line) for (a) fast disk (lower hardness) and (b) slow disk (higher hardness). (For interpretation of the references to colour in this figure legend, the reader is referred to the web version of this article.)

23.0 μm, demonstrating again that the majority of surface modification takes place on the less hard surface. Following load stage 4, the mean asperity radii were 130.0 μm and 24.2 μm for the less hard and harder surfaces, respectively, evolving to 145.4 μm and 24.8 μm after load stage 5.

In a similar manner to that presented for the disks of equal hardness, surface height distributions have been calculated and the relevant parameters are shown in Table 4.

From Table 4, it is again apparent that the majority of the surface modification during running-in takes place very rapidly, during the first load stage. Subsequent changes to the height distribution parameters for both disks are insignificant in comparison to the change which occurs during the first load stage.

Fig. 9 shows the histogram of surface heights for the initial fast disk surface (lower hardness), and for the same surface following load stages 1 and 5. The initial distribution in Fig. 9(a) can be seen to align closely with the superimposed Gaussian distribution curve. Following the first load stage, the histogram in Fig. 9(b) shows that a large amount of modification has occurred, predominantly to asperity tips. This can be seen by the reduction in the positive tail of the histogram. As a result of tip modifications, positive measurements become less widely distributed so that the high points of the profile are much closer to the mean. The negative tail of the histogram however has not changed significantly.

Further histograms such as that shown in Fig. 9(c) for load stage 5 demonstrate only very subtle changes occurring between load stages 1 and 5. Despite the changes occurring to the asperity tips, the negative tail of the distribution curve remains relatively stable and unchanging between load stages. This demonstrates that the wear and plastic deformation processes occur at the tips

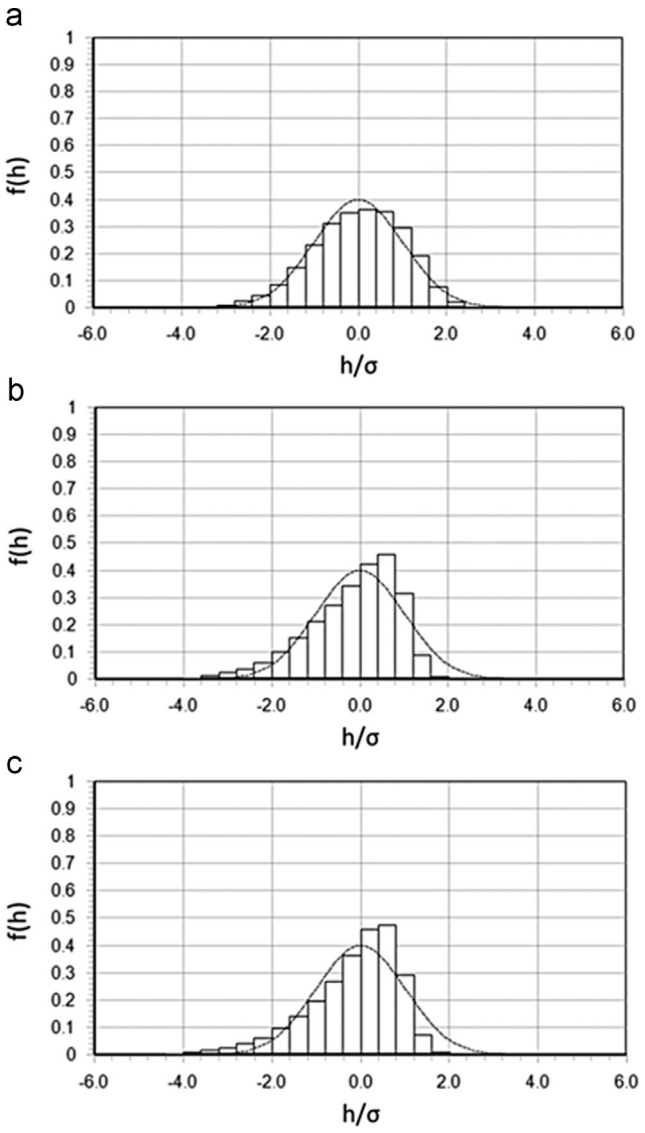

Fig. 9. Histogram of surface heights for fast disk (a) for un-run surface, (b) following load stage 1 and (c) following load stage 5.

Table 4
Roughness distribution data for disks of different hardness.

Load Stage	Disk	Standard deviation (μm)	Skewness
Unrun	Fast	0.295	−0.291
	Slow	0.479	−0.734
1	Fast	0.231	−0.829
	Slow	0.448	−1.028
2	Fast	0.220	−0.964
	Slow	0.458	−1.068
3	Fast	0.220	−0.985
	Slow	0.450	−1.038
4	Fast	0.219	−1.044
	Slow	0.454	−1.014
5	Fast	0.215	−1.050
	Slow	0.451	−1.034

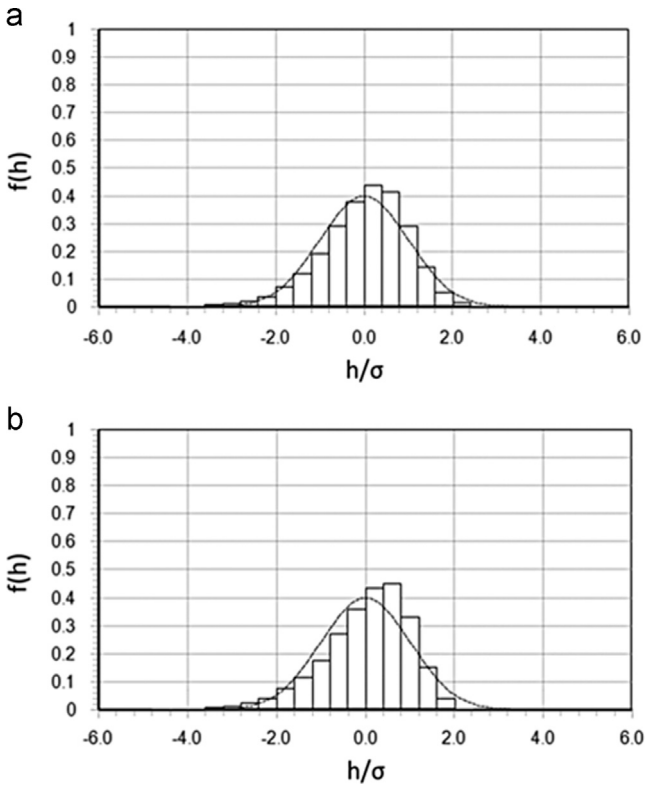

Fig. 10. Histogram of surface heights for slow disk (a) for un-run surface, (b) following load stage 5.

of the asperity features. Average roughness values show some change due to wear between load stages, but the overall shape of the distribution which has been generated by the initial plastic deformation processes remains consistent.

Considering the harder, slow disk surface, the realigned profiles show that little change has occurred during the running-in process. This is confirmed by the height distributions of the surface which show little variation, with only the most extreme features becoming more rounded and the distribution maintaining a slightly negatively-skewed Gaussian appearance. This is demonstrated clearly in Fig. 10, where height distributions for the surface following load stage 5 are very similar to the height distribution of the as-manufactured surface, with changes in the distribution being limited to a reduction in height of the most aggressive asperities.

It is therefore clear that, in surfaces of differing hardness, the running-in process still occurs rapidly, but the plastic deformation is concentrated on the surface of lower hardness. This reinforces the authors' view that running in is a process whereby a *pair* of surfaces tend to conform to each other.

5. Observations of micropitting in disk surfaces of equal hardness

Once the surfaces had been run-in via the procedure outlined here, they were subsequently used for a series of experiments investigating mixed lubrication [18]. Following some 850,000 fast disk rotational cycles, the running tracks of the pair of disks of equal hardness became matted in appearance. This is known to indicate micropitting, and is clearly evident in Fig. 11.

Upon removing the disks from the rig and measuring the surfaces, it was clear that micropitting had altered the surface texture at the microscale on both test surfaces. It is also clear from Fig. 11 that narrow reflective regions of surface are present on either side of the central micropitted region, and it is the authors' view that these are

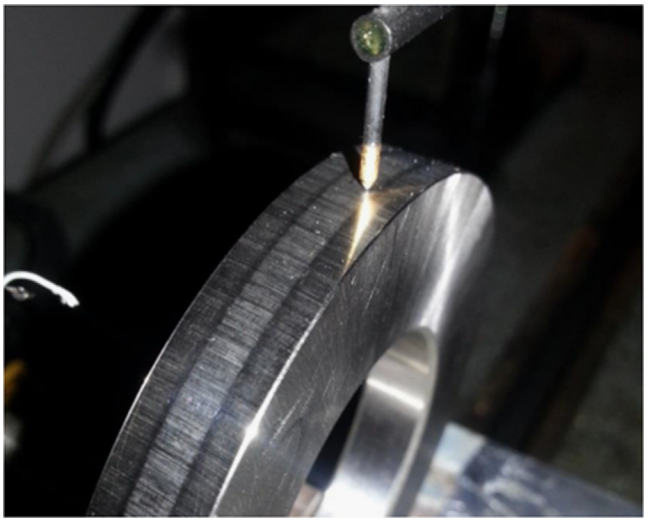

Fig. 11. Fast disk from equal hardness pair, showing central matted running track.

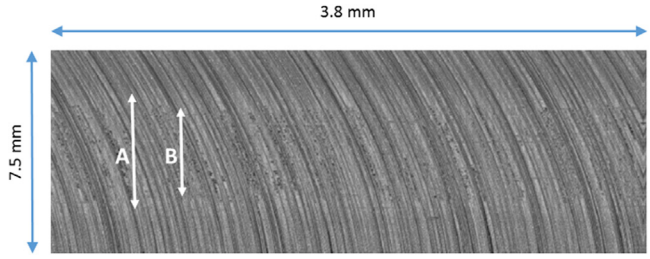

Fig. 12. 3-d surface profilometer measurement of micropitted running track.

the result of plastic deformation in the absence of fatigue failure. The initial running-in tests reported here were run at high load for a low number of load cycles and would have created a wider running track than the subsequent lower load mixed lubrication tests [18], but the low number of cycles in this region would not have been sufficient to initiate any kind of fatigue damage. This can be further seen in Fig. 12, which is a photo-simulation of a portion of running track produced from three-dimensional surface roughness measurements taken using a profilometer fitted with a *y*-stage. Arrows A and B indicate the approximate widths of the running track during the running in tests, and the micropitted region respectively.

It should be noted that the distorted aspect ratio (for clarity of presentation) of Fig. 12 exaggerates the sweep of the roughness resulting from the crown grinding of the disks. If shown with an undistorted aspect ratio, the grinding marks are seen to be aligned at approximately 4° to the shaft axis within the contact area.

Micropitting appears to be distributed relatively evenly across the running tracks. This indicates that it is not driven by the nominal Hertzian pressure which falls from a maximum value at the centre of the disks to less than 10% of that value at the extremes of arrow B in Fig. 12. It is likely, however, that it is driven by the pressure loading applied to the asperity features which persists to the edges of the contact. The most severe asperity loading in elliptical contacts has been found to occur at the extreme edges of the contact zone [23]. As a result the even distribution may be due to the fact that the harshest loading experienced at the outer edges occurs less frequently as load is reduced and the contact area decreases, whereas the central region sees the lower rate of contact occurrence but with damage accumulated over all the loads used in the mixed lubrication tests.

An enlarged section of Fig. 12 may be seen in Fig. 13 where the dependency of the fatigued region on roughness can be seen. Micropits appear distributed across prominent roughness ridges.

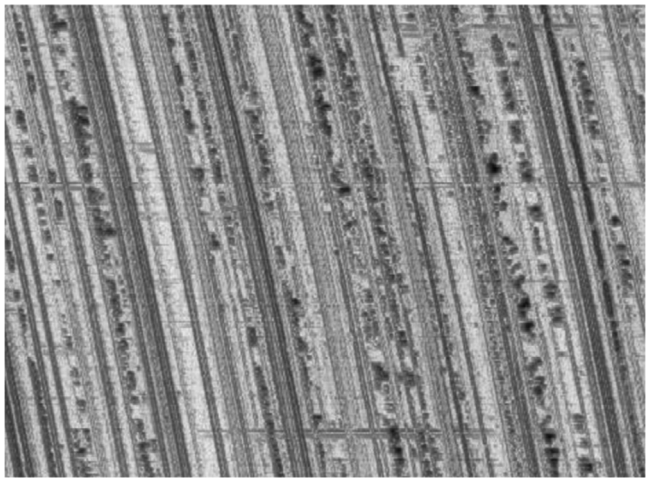

Fig. 13. Enlarged view of micropitted running track (dimensions are approximately 0.5 mm in circumferential direction × 1.2 mm in axial direction).

Where micropitting has occurred, due to the nominally extruded nature of the finish, it appears to have occurred across the whole ridge of an asperity. Prominent ridges appear to show micropits occurring very densely across the scan. It can be clearly seen that neighbouring asperity ridges do not show the same level of pitting, and that there is no indication of pits occurring within valley features. Results shown in Section 3 demonstrate that interaction between surfaces occurs predominantly at the most prominent asperity tips, where modification and plastic deformation occurs.

Both disks showed similar features, with micropits clearly associated with asperities. This is most clearly demonstrated by comparison of relocated surface roughness profiles measured from the fatigued surfaces with those taken from the as-manufactured and stable, run-in surfaces. Such a comparison is shown in Fig. 14. When realigned with the un-run surface, it appears that asperity features which undergo large initial plastic deformation are at risk of damage. An example of this can be seen where at $x=0.24$ mm (marked A) where a very prominent asperity feature on the un-run profile is flattened by approximately 0.7 μm during running-in. Sustained running of the profile resulted in the creation of a valley with a depth of $z=-0.91$ μm. Relocated profiles from the surfaces very clearly demonstrate the strong relationship between the location of surface pits and initial prominent asperity features. Furthermore – realigning fatigued profiles with the un-run surface appears to demonstrate a relationship between the most severely plastically deformed regions during running-in and subsequent locations of surface fatigue, although this will also be influenced by their retained prominence in the contact. The link between high levels of plastic deformation of asperities and subsequent micropitting, would support the observations of Bryant et al. [15] who demonstrated that residual tensile stresses result from asperity plastic deformation, which would make heavily deformed asperities more susceptible to fatigue failure [24]. However, it must be noted that the authors are presenting this observation simply as one of many potential contributory factors to the complex phenomenon of micropitting in lubricated contacts [25].

6. Conclusions

From this work, which investigated hardened steel surfaces operating under mixed lubrication conditions typical of gear teeth, it can be concluded that:

- Running-in is a rapid process, where the tips of asperities are plastically deformed in the first few cycles of loading

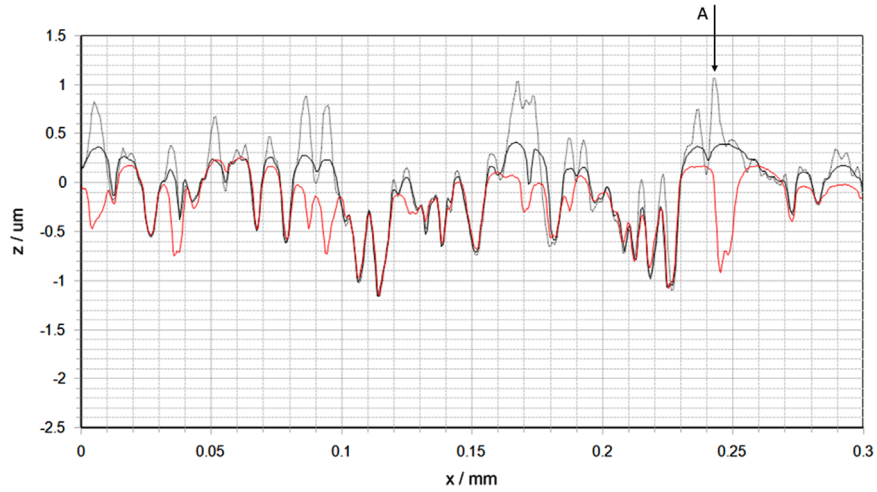

Fig. 14. Relocated profiles from micropitted slow disk, showing original as-manufactured profile (grey), stable surface after running-in (black) and the micropitted surface (red). (For interpretation of the references to colour in this figure legend, the reader is referred to the web version of this article.)

- Valley features remain unchanged by the process, and asperity tips become flattened, negatively skewing the asperity height distributions
- Once run-in, surface pairs are stable unless their relative alignment or their operating conditions (and hence film thickness and asperity contact pressures) change.
- For surfaces in contact which are not of similar hardness, the bulk of the plastic deformation during running-in occurs on the surface with lower hardness. However surface modification is still limited to the asperity tips of that surface
- Plastic deformation during running in appears, in the samples examined, to be a contributory factor to subsequent micropitting failure of the surfaces. In these samples, micropits appear to form at the position of asperity features which were prominent in the original, un-run surface and experienced significant plastic deformation during running-in.

Data access statement

Information on how to access the data that supports the results presented in this article can be found in the Cardiff University data catalogue at http://dx.doi.org/10.17035/d.2016.0008118727.

Acknowledgements

The authors wish to acknowledge the support of the British Gear Association, and EPSRC Grant references EP/L021757/1, and EP/K031635/1 which facilitated this work in part. Support was also received from the Austrian Research Promotion Agency (FFG) within the framework of the COMET K2 Excellence Center of Tribology (X-Tribology). The funders have not in any way influenced the content of this paper.

References

[1] Hutchings IM. Tribology: friction and wear of engineering materials. Butterworth: Heinemann; 1992.
[2] Abbott EJ, Firestone FA. Specifying surface quality – a method based on accurate measurement and comparison. J Mech Eng 1933;55:569–72.
[3] Blau PJ. On the nature of running in. Tribol Int 2005;38:1007–12.
[4] Halling J. Principles of tribology. United Kingdom: Macmillan; 1975.
[5] Whitehouse DJ, Archard JF. The properties of random surfaces of significance in their contact. Proc R Soc Lond A: Math Phys Sci 1970;316:97–121.
[6] Bishop, IF, Snidle, RW. An investigation of alternative methods of quantifying running-in of surfaces. Society of Automotive Engineers, 1984, Paper No. 840100, presented at SAE International Congress and Exposition, Detroit; 1984.
[7] Østvik, R, Christensen, H. Changes in surface topography with running-in. In: Proceedings of the Institution of Mechanical Engineers, Conference Proceedings, 183; 1968. p. 57–65.
[8] Barber GC, Lee JC, Ludema KC. Materials and surface finish effects in the breaking-in process of engines. J Eng Gas Turbines Power 1987;109:380–7.
[9] Lord J, Larsson R. Film-forming capability in rough surface EHL investigated using contact resistance. Tribol Int 2008;41:831–8.
[10] Andersson S. Initial wear of gears. Tribol Int 1977;10:206–10.
[11] Bishop, IF, Snidle, RW. Running-in of ground surfaces under elastohydrodynamic conditions. Paper No. 830310, in Special Publication 539, Studies of engine bearings and lubrication, Society of Automotive Engineers, Warrendale; 1983. p. 53–64.
[12] Bishop IF, Snidle RW. Some experimental aspects of running-in and scuffing failure of steel discs operating under elastohydrodynamic conditions. In: Downson D, et al., editors. The running-in process in tribology. United Kingdom: Butterworth-Heinemann; 1982.
[13] Tudor GK. An electrical method of investigating the lubrication in a journal bearing. J C.S.I.R (Austral.) 1948;21:202–9.
[14] Lohner T, Mayer J, Michaelis K, Höhn B-R, Stahl K. On the running-in behavior of lubricated line contacts. Proc Inst Mech Eng Part J: J Eng Tribol 2015.
[15] Bryant MJ, Evans HP, Snidle RW. Plastic deformation in rough surface line contacts – a finite element study. Tribol Int 2012;46:269–78.
[16] Oila A. Micropitting and related phenomena in case carburised gears (Ph.D. thesis). United Kingdom: Newcastle Univesity; 2003.
[17] Weeks IJJ. An experimental investigation into the mixed lubrication of steel surfaces (Ph.D. thesis). United Kingdom: Cardiff University; 2015.
[18] Clarke A, Weeks I, Evans HP, Snidle RW. An investigation into mixed lubrication conditions using electrical contact resistance techniques. Tribol Int 2016;93 B:709–16.
[19] Holmes MJA, Qiao H, Evans HP, Snidle RW. Surface contact and damage in micro-EHL. In: Dowson D, et al., editors. Tribology and interface engineering series. United Kingdom: Elsevier; 2005.
[20] Jamari J, Schipper DJ. Deterministic repeated contact of rough surfaces. Wear 2007;264:349–58.
[21] Cabanettes F, Rosén B-G. Topography changes observation during running-in of rolling contacts. Wear 2014;315:78–86.
[22] Rowe GW, Kaliszer H, Trmal G, Cotter A. Running-in of plain bearings. Wear 1975;34:1–14.
[23] Holmes MJA, Evans HP, Snidle RW. Analysis of mixed lubrication effects in simulated gear tooth contacts. Trans ASME: J Tribol 2005;127:61–9.
[24] Clarke A, Evans HP, Snidle RW. Understanding micropitting in gears. Proc Inst Mech Eng Part C: J Mech Eng Sci 2015.
[25] Oila A, Bull SJ. Assessment of the factors influencing micropitting in rolling/sliding contacts. Wear 2005;258:1510–24.